Very large plasmon band shift in strongly coupled metal nanoparticle chain arrays.

L. A. Sweatlock[1], J. J. Penninkhof[2], S. A. Maier[1], A. Polman[2], and H. Atwater[1]
[1]Thomas J. Watson Laboratories of Applied Physics, Caltech
Pasadena, CA 91125, USA
[2]FOM Institute for Atomic and Molecular Physics (AMOLF)
Kruislaan 407, 1098 SJ Amsterdam, The Netherlands

Abstract

30 MeV silicon ion irradiation of silica glass containing 10 nm silver nanocrystals causes alignment of the nanocrystals in closely spaced linear arrays along the ion tracks. Optical transmission measurements show a 1.5 eV splitting of the surface plasmon resonant absorption bands for polarizations longitudinal and transversal to the arrays. The resulting material is a highly anisotropic glass that absorbs blue light of one polarization, and near-infrared light of the orthogonal polarization. Finite-difference time domain simulations are used to explore the effects of interparticle spacing and total array length on the absorption properties.

Introduction

The optical extinction properties of small metal particles have been studied for many years [1, 2]. Noble metal nanoparticles embedded in a dielectric exhibit a strong absorption peak due to a collective motion of free electrons, that is, a surface plasmon resonance. For isolated spherical particles, the resonance peak occurs generally in the visible part of the spectrum. The particular frequency depends on the particle size, and the dielectric constants of the metal and of the surrounding medium. For particle ensembles, however, electromagnetic coupling between neighboring particles shifts the plasmon absorption bands [3]. Numerical calculations have demonstrated that nanoparticle size, nearest neighbor spacing, and the overall ensemble size and shape have a critical effect on extinction spectra [4].

In linear arrays of particles the optical response is anisotropic, since the character of interparticle coupling depends on whether incident light is polarized longitudinal or transversal to the chain axis. In particular, the longitudinal collective extinction resonance can be significantly red-shifted throughout the technologically relevant visible and near-infrared spectrum. Wavelength tuning is achieved by engineering the strength of interparticle coupling. The transverse mode extinction is modestly shifted to higher frequencies.

It has been experimentally demonstrated that nanoparticle chains are capable of guiding electromagnetic energy via dipolar near-field interactions comparable to Forster transfer [5]. These structures exhibit lateral mode confinement smaller than the optical diffraction limit, which cannot be achieved with conventional waveguides [6], nor with other novel technologies such as photonic crystals [7] or plasmonic stripe waveguides [8]. Therefore metal nanoparticle chains are of interest for applications in photonics

where local concentration of electromagnetic fields is critical, including nonlinear devices and sensors.

We have previously explored nanoparticle arrays fabricated by electron beam lithography with 50 nm particles and 25 nm next-neighbor spacing. [5, 9] Motivated by potential technological applications, we consider shrinking these length scales in order to increase the strength of interparticle coupling. In this note we discuss an experimental method for producing quasi-ordered arrays of 10 nm particles spaced by 2 nm or less. We then connect the experimental far-field optical extinction results with finite-difference time domain (FDTD) simulations.

Method

Our collaborators have shown that anisotropic core-shell particles can be fabricated by megaelectron-volt (MeV) ion irradiation of colloidal spheres consisting of a metal core surrounded by a silica shell [10]. The shape change of the metal core is attributed to an anisotropic deformation of the silica matrix, which is known to occur in amorphous materials [11]. This led us to investigate the effect of MeV ion irradiation on silver (Ag) nanocrystals in a glass film.

Ionic silver is introduced into sodalime glass by immersing the substrate into a melt of Ag salts. The silver replaces native sodium via an ion exchange interaction. Nucleation of Ag nanocrystals is induced by 1 MeV irradiation with xenon ions. These heavy, relatively low energy particles cause atomic displacements that enhance mobility of the embedded Ag. Nucleation could alternatively be accomplished by thermal annealing. Finally, the sample is exposed to 30 MeV silicon ions with an incident angle 60 degrees from normal, while cooled to a temperature of 77 K. Under these conditions the primary stopping mechanism for the energetic ions is electronic braking rather than atomic collisionrents. Electronic braking causes a thermal spike along the ion trajectory, which is thought to be responsible for anisotropic deformation of the matrix. No deformation of the individual particles is observed. Please refer to our recent letter [12] for additional information regarding our fabrication method.

An established method for fabricating optically dichroic glass is via ultrafast laser pulse deformation of embedded Ag nanoparticles [13]. Intense femtosecond optical pulses are found to induce various morphological changes to the Ag nanoclusters [14]. In contrast, the ion irradiation procedure we propose in this report induces plastic flow in the glass matrix, and results in the ordering of particles into chain arrays without noticeably altering the morphology of individual particles. The two methods produce significantly different nanostructure as well as distinct optical extinction spectra, and each promises interesting technical applications.

Results

Optical extinction is determined by normal-incidence transmission spectroscopy for polarizations parallel and perpendicular to the projection of the ion trajectories onto

the surface. Also, plan-view TEM samples were prepared via ion milling with a kiloelectron-volt argon beam.

Figure 1 (a & b): TEM of samples before (a) & after (b) high energy ion irradiation. Inset, FFT of image confirms particle orientation along ion tracks.

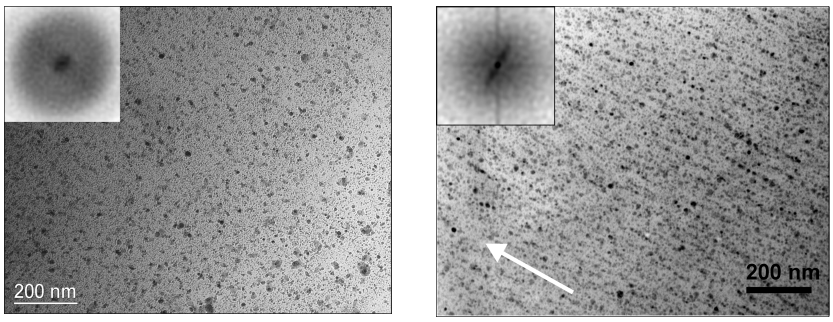

Normal incidence plan-view TEM images appear in Figure 1. The first panel shows Ag particles with diameters typically in the range 2-15 nm, dispersed throughout the glass after annealing with 1 MeV Xe ions. Particles appear to be randomly arranged throughout the matrix, and indeed, the inset spatial fast fourier transform (FFT) of the image shows no directionality. The second panel shows the sample following high-energy Si irradiation, with the direction of the ion tracks indicated by an arrow. In this case, quasi-linear arrays of nanoparticles are observed, and FFT confirms that the arrays are oriented parallel to the ion beam.

Figure 2. Optical extinction of Ag nanoparticles in BK7-type glass irradiated with 30 MeV Si, including optical polarizations longitudinal ("s-pol") and transversal ("p-pol") to the projection of the ion beam direction into the normal plane. Also shown is the extinction of an isotropic control sample with randomly oriented nanoparticles (solid line) and with only unannealed ionic Ag (dashed line).

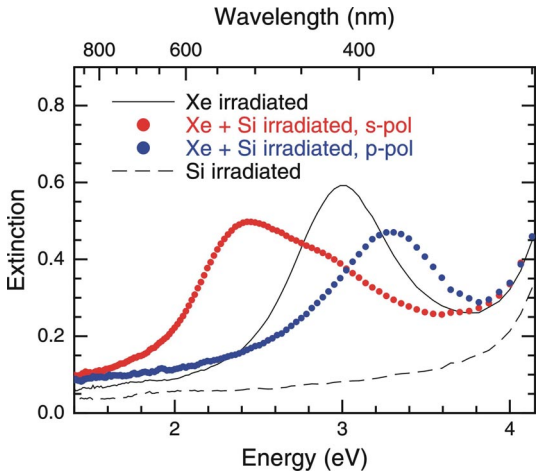

Figure 2 presents optical extinction spectra of the samples consisting of Ag nanoparticles in glass following irradiation with 30 MeV Si for optical polarizations longitudinal ("s-pol") and transversal ("p-pol") to the projection of the ion beam direction into the surface plane. A solid line indicates the isotropic response of an annealed sample without Si ion irradiation, which contains only randomly oriented nanoparticles. The broken line is the extinction of a sample containing only unannealed ionic Ag. In this typical example, the longitudinal plasmon extinction peak redshifts by 0.6 eV relative to the isotropic response of the control sample while the transversal peak blueshifts by a smaller amount. We have shown elsewhere [12] that the magnitude of the peak splitting can be tuned by controlling the total ion fluence. This result is summarized in Figure 3.

Figure 3.
Peak position [eV] of collective plasmon extinction resonance for Ag nanoparticles in BK7 glass irradiated with various fluences [1e15 ions/cm^2] of 30 MeV Si, including optical polarizations longitudinal (lower branch) and transversal (upper branch) to the projection of the ion beam into the normal plane. Particularly in the longitudinal direction, the resonance frequency is a strong function of fluence.

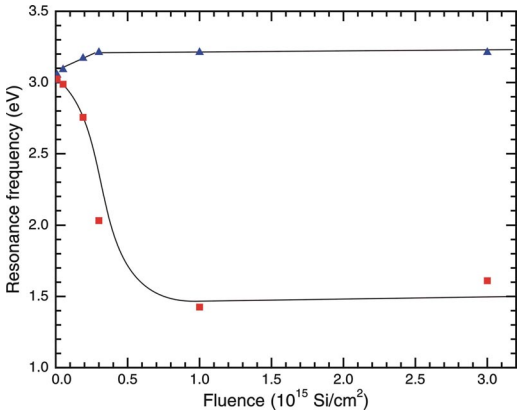

From literature results [4, 15], we understand that the dependence of resonance peak frequency on ion fluence may result from either a decreasing typical interparticle spacing, or from an increasing average nanoparticle chain length, or from a combination of several effects. We use FDTD simulation to understand the relative importance of these effects in idealized chains with critical dimensions similar to those observed in TEM. Simulations have the added benefit of helping bridge the gap between optical far-field extinction and interesting near-field effects, which would be challenging to address directly in experiment.

Because it is difficult to explicitly perform a simulation of frequency scanning spectroscopy with a time domain algorithm, a two-step process is used to simulate the plasmon resonance frequencies. First, the simulation volume is irradiated by a pulse with an off-resonance center frequency that allows the particle chain to absorb energy into any modes that may exist. The particles' relaxation is then observed in the time domain. Fourier transform of this data gives the frequency position of any resonant absorption peaks. Once the spectrum is outlined in this way, on-resonance excitation may be used to excite individual modes, for example, to examine the corresponding energy density profile.

Figure 4
Simulated longitudinal extinction spectra for four-particle chains of 10 nm Ag particles in glass with various interparticle spacings; and for comparison the simulated spectra of a single nanoparticle. Decreasing spacing leads to stronger interparticle coupling, and thus an increasing peak shift towards lower frequency.

Peaks of magnitude less than 1 are non-dipole modes, artifacts of the simulation mesh.

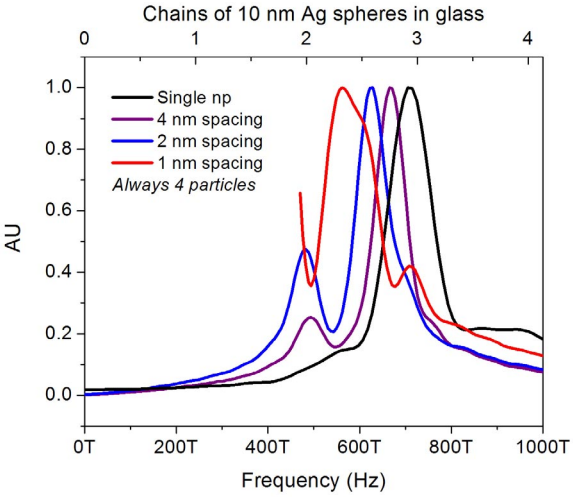

Figure 4 shows a simulated longitudinal polarization extinction spectrum for four-particle chains of 10 nm Ag particles. The particle size and chain length are chosen as

typical of chains observed in TEM. The data series in Figure 4 represent arrays with various interparticle spacings, and also isolated particles. The simulated peak for isolated particles at 2.9 eV is in good agreement with the experimental control, suggesting that the as-annealed sample consists of essentially uncoupled nanoparticles. Decreasing interparticle spacing leads to stronger coupling, and thus to a peak shift of increasing magnitude towards lower frequencies. Secondary peaks (with amplitude less than 1 in Figure 4) were investigated by selective excitation, and were found to correspond to non-dipole modes that occur as artifacts of the simulation mesh.

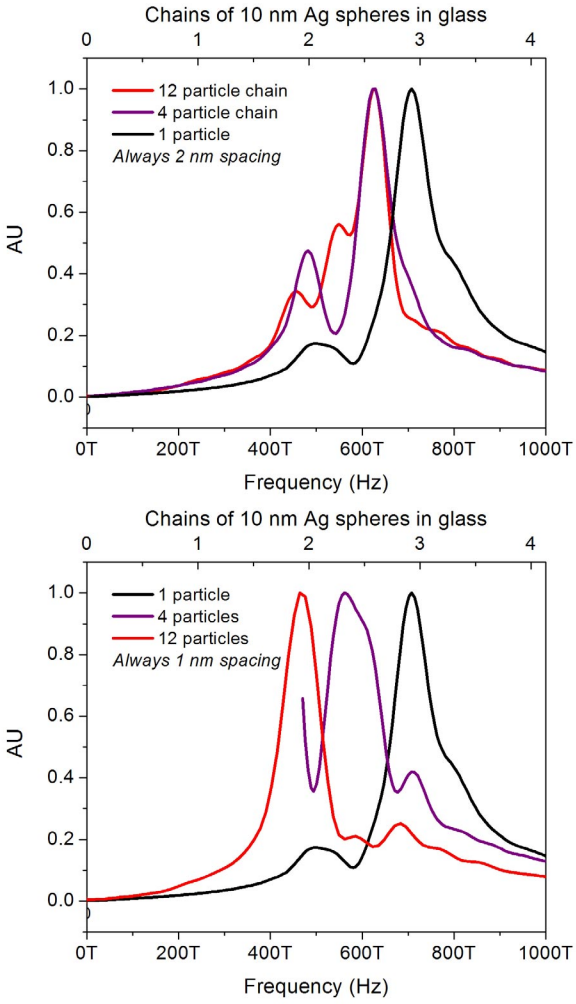

Figure 5
Simulated longitudinal extinction spectra for chains of 10 nm Ag particles in glass with fixed interparticle spacing and variable chain length; and for comparison the simulated spectra of a single nanoparticle.

Peaks of magnitude less than 1 are non-dipole modes, artifacts of the simulation mesh.

In panel (a), the spacing is fixed at 2 nm. In this case there is no difference between long and short chains of nanoparticles.

However in panel (b), the spacing is fixed at 1 nm. For this very close interparticle spacing, the particle chain length is also a critical parameter.

In Figure 5 the effect of total chain length on the extinction properties of Ag nanoparticle chains is explored, again considering only the longitudinal polarization. The two panels correspond to chains with interparticle spacing of 1 or 2 nm. In the first panel, the overall length of the array is not a critical factor. However, for the very close interparticle spacing seen in the second panel, the length of the array becomes an important parameter.

Discussion

Here we have demonstrated a method for fabrication of an exceptionally anisotropic bulk glass. The optical anisotropy results from resonant absorption into longitudinal and transverse collective plasmon modes in chains of silver nanoparticles. The longitudinal resonance can be tuned by 1.5 eV or more, throughout the visible and near infrared.

Comparison of finite element simulation with TEM images helps relate the material nanostructure to optical extinction. Although important questions still remain, we are progressing toward understanding the dynamics of the process by which ion irradiation leads to nanoparticle alignment. Simulation also allows connection between far-field measurements and near-field parameters such as local enhancement of electric field amplitudes that would be difficult to measure directly. Indeed, the very small length scales accessible by this fabrication technique suggest potential use in applications in which the local field amplitude is critical.

Acknowledgements

The authors would like to acknowledge A. Vredenberg (Utrecht University) and B. Kooi (University of Groningen), whose experimental expertise was an invaluable asset. Research supported by Air Force Office of Scientific Research, the Center for Science & Engineering of Materials at Caltech, and NWO in The Netherlands.

References

[1] Mie, G. *Ann. Phys*. **25,** 377-445 (1908).
[2] Kreibig, U. and M. Vollmer, Optical Properties of Metal Clusters. (Springer, 1995).
[3] Gérardy, J. M. and M. Ausloos, *PRB* **25**, 4204 (1982).
[4] Quinten, M. and U. Kreibig, *Appl. Opt*. **32**, 6173 (1993).
[5] Maier, S. A. et al., *Nature Materials* **2**, 229 (2003).
[6] Saleh, B. E. and M. C. Teich, Fundamentals of Photonics. (Wiley, 1991).
[7] Mekis, A. et al., *PRL* **77**, 3787-3790 (1996).
[8] Lamprecht et al., *APL* **79**, 51 (2001).
[9] Maier, S. A., P. G. Kik, and H. A. Atwater, *APL* **81**, 1714-1716 (2002).
[10] Roorda, S., T. van Dillen, C. Graf, A. M. Vredenberg, B. J. Kooi, A. van Blaaderen, and A. Polman, in press 2003.
[11] Snoeks, E., A. van Blaaderen, T. van Dillen, C. M. van Kats, M. L. Brongersma, and A. Polman, *Adv. Mat.* **12**, 1511 (2000).
[12] Penninkhof, J. J., L. A. Sweatlock, A. M. Vredenberg, B. J. Kooi, S. A. Maier, H. A. Atwater, and A. Polman, *APL* **83**, 4137 (2003).
[13] Kaempfe, M., T. Rainer, K.-J. Berg, G. Seifert, and H. Graener, *APL* **74**, 1200 (1999).
[14] Kaempfe, M., H. Hofmeister, S. Hopfe, G. Seifer, and H. Graener. *J. Phys. Chem. B* **2000**, 11847-11852.
[15] Lamprecht, B. et al., *PRL* **84**, 4721-4724 (2000).